

Comparison of symmetric and asymmetric bipolar type high triplet energy host materials for deep blue phosphorescent organic light-emitting diodes

Soon Ok Jeon and Jun Yeob Lee*

Received 7th February 2012, Accepted 9th February 2012

DOI: 10.1039/c2jm30742a

Symmetric and asymmetric bipolar host materials for deep blue phosphorescent organic light-emitting diodes were developed and the chemical structure of the host materials was correlated with the device performances. The bipolar host with the asymmetric molecular structure was better than the host with symmetric molecular structure in terms of driving voltage and quantum efficiency due to better charge transport properties. A high quantum efficiency of 24.5% and a high power efficiency of 31.0 lm W⁻¹ were achieved in the deep blue device using the asymmetric bipolar host due to balanced charge transport and low driving voltage.

Introduction

The development of high efficiency deep blue phosphorescent organic light-emitting diodes (PHOLEDs) is important because the power consumption of organic light-emitting diodes (OLEDs) can be greatly reduced by using the deep blue PHOLEDs instead of current deep blue fluorescent OLEDs. However, the quantum efficiency of the deep blue PHOLEDs should be improved further and the development of the materials and device architecture is required.

There have been many studies to improve the quantum efficiency of deep blue PHOLEDs and most research was focused on developing host and dopant materials. Several deep blue dopant materials based on carbene,^{1–3} pyridine triazolates⁴ and halogen substituted phenylpyridine^{5,6} were synthesized and a deep blue color coordinate could be obtained from those deep blue dopant materials. Various host materials were also synthesized, which include carbazole derivatives,^{7–9} silane derivatives,^{10,11} and phosphine oxide derivatives.^{12–17} Carbazole derivatives were generally used as the host material for deep blue PHOLEDs, but they suffer from poor electron injection due to strong hole transport properties of the carbazole.⁷ Several silane type materials were also synthesized, but they had a problem of poor hole injection in spite of high triplet energy.^{10,11} Phosphine oxide type compounds were also effective as high triplet energy hosts for deep blue PHOLEDs.^{13–15} The merit of the phosphine oxide materials was to improve the electron transport properties of the core structure. Bipolar type phosphine oxide derivatives with carbazole based core structures could improve the maximum quantum efficiency of deep blue PHOLEDs up to the theoretical limit of quantum efficiency.^{14,15} Other than these materials, several bipolar type

high triplet energy host materials were also reported and high efficiency was obtained.^{18–22} Although several high triplet energy bipolar host materials have been developed for deep blue PHOLEDs, there have been few systematic studies to correlate the molecular structure of the host materials with the device performances of deep blue PHOLEDs. The correlation of the molecular structure with the device performances is important to design high triplet energy host materials for high quantum efficiency in deep blue PHOLEDs. In particular, the driving voltage of the deep blue PHOLEDs was high due to the wide bandgap of the host material and large energy barrier for charge injection. Therefore, it is strongly required to develop new host materials which can lower the driving voltage and enhance the quantum efficiency over 20% through novel molecular design of the host materials.

In this work, novel bipolar type high triplet energy host materials with symmetric and asymmetric molecular structures were developed and their device performances were investigated. The symmetric and asymmetric host materials were compared in terms of photophysical properties and device performances. It was demonstrated that the asymmetric molecular structure is better than the symmetric molecular structure to improve the driving voltage and quantum efficiency of the deep blue PHOLEDs. A high maximum quantum efficiency of 24.5% and low driving voltage of 6.5 V at 1000 cd m⁻² were achieved using the asymmetric host material.

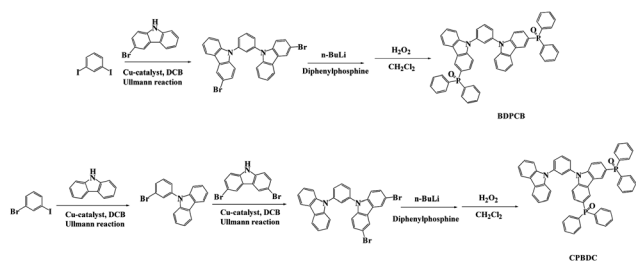
Experimental section

Synthesis

The synthetic scheme of the host material is shown in Scheme 1.

Synthesis of 1,3-bis(3-bromo-9H-carbazole-9-yl)benzene. 1,3-Diiodobenzene (4.00 g, 12.1 mmol), 3-bromo-9H-carbazole (6.56 g, 26.6 mmol), potassium carbonate (13.4 g, 96.9 mmol), Cu

Department of Polymer Science and Engineering, Dankook University, 126, Jukjeon-dong, Suji-gu, Yongin, Gyeonggi, 448-701, Republic of Korea. E-mail: leej17@dankook.ac.kr; Fax: +82 31 8005 3585; Tel: +82 31 8005 3585



Scheme 1 Synthetic scheme of BCPCB and CPBDC.

powder (3.08 g, 48.4 mmol) and dibenzo 18-crown-6 (0.64 g, 2.42 mmol) were dissolved in anhydrous *o*-dichlorobenzene under nitrogen atmosphere. The reaction mixture was stirred for 12 h at 100 °C. The mixture was diluted with dichloromethane and washed with distilled water (100 mL) three times. The organic layer was dried over anhydrous magnesium sulfate and evaporated *in vacuo* to give the crude product, which was purified by column chromatography by *n*-hexane. The final white powdery product was obtained in 90% yield. ¹H NMR (500 MHz, CDCl₃): δ 8.22 (s, 2H), 8.12 (d, 2H, *J* = 7.7 Hz), 8.05 (d, 2H, *J* = 8.0 Hz), 7.82 (t, 2H, *J* = 7.9 Hz), 7.68–7.62 (m, 3H), 7.53–7.22 (m, 7H). ¹³C NMR (125 MHz, CDCl₃): δ 141.1, 139.2, 131.7, 129.1, 127.1, 126.4, 126.2, 125.3, 123.5, 122.7, 121.0, 120.9, 120.6, 113.4, 110.0, 109.8. MS (FAB) *m/z* 566 [(M + H)⁺]. Anal. calcd for C₁₈H₃₀Br₂N₂: C, 63.63; H, 3.20; N, 4.95. Found: C, 63.32; H, 3.53; N, 4.94.

Synthesis of 1,3-bis(3-(diphenylphosphoryl)-9H-carbazole-9-yl)benzene (BCPCB). Into a 100 mL, two-neck flask was placed 1,3-bis(3-bromo-9H-carbazole-9-yl)benzene (2.00 g, 3.53 mmol) in tetrahydrofuran (30 mL). The reaction flask was cooled to –78 °C and *n*-butyllithium (2.5 M in hexane, 3.53 mL) was added dropwise slowly. The whole solution was stirred at this temperature for 3 h, followed by addition of a solution of chlorodiphenylphosphine (1.94 g, 8.82 mmol) under argon atmosphere. The resulting mixture was gradually warmed to ambient temperature and quenched by methanol (10 mL). The mixture was extracted with dichloromethane. The organic layers were dried over magnesium sulfate, filtered, and evaporated under reduced pressure. The white powdery product was obtained to 1.14 g.

A mixture of 1,3-bis(3-(diphenylphosphino)-9H-carbazole-9-yl)benzene, dichloromethane (20 mL), and hydrogen peroxide (4 mL) was stirred overnight at room temperature. The organic layer was separated and washed with dichloromethane and water. The extract was evaporated to dryness affording a white solid. The final product was purified by sublimation. Overall yield: 40%. *T_g* 146 °C. ¹H NMR (500 MHz, CDCl₃): δ 8.65 (d, 2H, *J* = 12.2 Hz), 8.11 (d, 2H, *J* = 7.8 Hz), 7.86 (t, 1H, *J* = 7.9 Hz), 7.81–7.75 (m, 10H), 7.70–7.66 (m, 3H), 7.59–7.57 (m, 2H), 7.52–7.50 (m, 6H), 7.46–7.43 (m, 10H), 7.31–7.28 (t, 2H, *J* = 7.4 Hz). ¹³C NMR (125 MHz, CDCl₃): δ 142.3, 141.0, 138.6, 133.5, 132.7, 132.0, 131.9, 131.8, 129.5, 129.4, 128.4, 128.3, 127.0, 126.4, 125.3, 125.1, 123.7, 123.5, 122.9, 122.6, 121.2, 120.8, 109.8, 109.7, 109.6. MS (FAB) *m/z* 808 [(M + H)⁺]. Anal. calcd for C₅₄H₃₈N₂O₂P₂: C, 80.19; H, 4.74; N, 3.46. Found: C, 80.25; H, 4.70; N, 3.28.

Synthesis of 9-(3-(9H-carbazole-9-yl)phenyl)-3,6-dibromo-9H-carbazole. 9-(3-Bromophenyl)-9H-carbazole (4.75 g, 14.7 mmol), 3,6-dibromo-9H-carbazole (4.00 g, 12.3 mmol), potassium carbonate (6.80 g, 49.2 mmol), Cu powder (1.56 g, 24.6 mmol) and dibenzo 18-crown-6 (0.97 g, 3.69 mmol) were dissolved in anhydrous *o*-dichlorobenzene under nitrogen atmosphere. The reaction mixture was stirred for 12 h at 100 °C. The mixture was diluted with dichloromethane and washed with distilled water (100 mL) three times. The organic layer was dried over anhydrous MgSO₄ and evaporated *in vacuo* to give the crude product, which was purified by column chromatography by *n*-hexane. The final white powdery product was obtained in 90% yield.

Yield 90%. ¹H NMR (500 MHz, CDCl₃): δ 8.16 (s, 2H), 8.13 (d, 2H, *J* = 7.7 Hz), 7.82 (t, 1H, *J* = 7.9 Hz), 7.73–7.69 (m, 2H), 7.58 (d, 1H), 7.51–7.48 (m, 4H), 7.44–7.41 (m, 2H), 7.35–7.29 (m, 4H). ¹³C NMR (125 MHz, CDCl₃): δ 140.7, 139.9, 139.8, 128.6, 131.7, 129.9, 126.7, 126.4, 125.8, 125.4, 124.4, 123.9, 123.6, 120.7, 113.7, 111.6, 109.7. MS (FAB) *m/z* 566 [(M + H)⁺]. Anal. calcd for C₁₈H₃₀Br₂N₂: C, 63.63; H, 3.20; N, 4.95. Found: C, 63.70; H, 3.32; N, 4.94.

Synthesis of 9-(3-(9H-carbazole-9-yl)phenyl)-3,6-bis(diphenylphosphoryl)-9H-carbazole (CPBDC). Into a 100 mL, two-neck flask was placed 9-(3-(9H-carbazole-9-yl)phenyl)-3,6-dibromo-9H-carbazole (4) (2.06 g, 3.63 mmol) in tetrahydrofuran (30 mL). The reaction flask was cooled to –78 °C and *n*-butyllithium (2.5 M in hexane, 3.63 mL) was added dropwise slowly. The whole solution was stirred at this temperature for 3 h, followed by addition of a solution of chlorodiphenylphosphine (2.00 g, 9.09 mmol) under argon atmosphere. The resulting mixture was gradually warmed to ambient temperature and quenched by methanol (10 mL). The mixture was extracted with dichloromethane. The organic layers were dried over magnesium sulfate, filtered, and evaporated under reduced pressure. The white powdery product was obtained and then a total of 9-(3-(9H-carbazole-9-yl)phenyl)-3,6-bis(diphenylphosphino)-9H-carbazole, dichloromethane (20 mL), and hydrogen peroxide (4 mL) were stirred overnight at room temperature. The organic layer was separated and washed with dichloromethane and water. The extract was evaporated to dryness affording a white solid. The final product was purified by sublimation.

Overall yield 60%. ¹H NMR (500 MHz, CDCl₃): δ 8.50 (d 2H, *J* = 12.2 Hz), 8.13 (d, 2H, *J* = 7.7 Hz), 7.87 (t, 1H, *J* = 7.9 Hz), 7.79–7.75 (m, 4H), 7.72–7.66 (m, 8H), 7.60–7.58 (m, 2H), 7.55–7.52 (m, 4H), 7.49–7.40 (m, 13H), 7.29 (t, 2H, *J* = 7.4 Hz). ¹³C NMR (500 MHz, CDCl₃): δ 143.5, 140.9, 140.2, 138.3, 133.7, 132.9, 132.6, 132.1, 130.8, 129.1, 127.5, 126.7, 126.2, 125.8, 125.0, 124.1, 123.5, 121.0, 110.6, 109.9. MS (FAB) *m/z* 808 [(M + H)⁺]. Anal. calcd for C₅₄H₃₈N₂O₂P₂: C, 80.19; H, 4.74; N, 3.46. Found: C, 80.13; H, 4.73; N, 3.40.

Device preparation and measurements

The device structure of blue PHOLEDs was indium tin oxide (ITO, 150 nm)/*N,N'*-diphenyl-*N,N'*-bis[4-(phenyl-*m*-tolyl-amino)-phenyl]-biphenyl-4,4'-diamine (DNTPD, 60 nm)/*N,N'*-di(1-naphthyl)-*N,N'*-diphenylbenzidine (NPB, 10 nm)/*N,N'*-dicarbazolyl-3,5-benzene (mCP, 10 nm)/BCPCB or CPBDC: bis((3,5-difluoro-4-cyanophenyl)pyridine) iridium picolate

(FCNirpic) (30 nm, 10%)/diphenylphosphine oxide-4-(triphenylsilyl)phenyl (TSPO1, 15 nm)/LiF (1 nm)/Al (200 nm). The device was further optimized and the blue PHOLED with poly(3,4-ethylenedioxythiophen):polystyrenesulfonate (PEDOT:PSS) and 25 nm thick TSPO1 layer was also fabricated. The device configurations of the hole only and electron only devices were ITO/DNTPD (60 nm)/NPB (10 nm)/mCP (10 nm)/BCPCB or CPBDC (30 nm)/Au (100 nm) and ITO/TSPO1 (10 nm)/BCPCB or CPBDC (30 nm)/TSPO1 (25 nm)/LiF (1 nm)/Al (100 nm). The device performances of the blue PHOLEDs were measured with a Keithley 2400 source measurement unit and a CS1000 spectroradiometer.

The ^1H nuclear magnetic resonance (NMR) and ^{13}C NMR spectra were recorded on a Varian 500 (500 MHz) spectrometer. The photoluminescence (PL) spectra were recorded on a fluorescence spectrophotometer (HITACHI, F-7000) and the ultraviolet-visible (UV-Vis) spectra were obtained by means of a UV-Vis spectrophotometer (Shimadzu, UV-2501PC). The differential scanning calorimetry (DSC) measurements were performed on a Mettler DSC 822 under nitrogen at a heating rate of $10^\circ\text{C min}^{-1}$. The mass analysis was performed using a JEOL, JMS-AX505WA spectrometer in fast atom bombardment mode. Photophysical properties of the material were analyzed using UV-Vis and PL spectrometer. BCPCB was dissolved in tetrahydrofuran at a concentration of 1.0×10^{-4} M for UV-Vis and PL measurements. Triplet energy analysis was carried out using the low temperature PL measurement in liquid nitrogen. Energy levels were measured using cyclic voltammetry (CV). The CV measurement of organic materials was carried out in acetonitrile solution with tetrabutylammonium perchlorate at 0.1 M concentration. Ag was used as the reference electrode and Pt was the counter electrode. Organic materials were coated on an indium tin oxide substrate and were immersed in an electrolyte for analysis. Ferrocene was used as the standard material for the CV measurement. Elemental analysis of the materials was carried out using an EA1110 (CE instrument).

Results and discussion

BCPCB and CPBDC were synthesized by the reaction of brominated carbazole with chlorodiphenylphosphine followed by the oxidation with hydrogen peroxide (Scheme 1). BCPCB had a symmetric molecular structure with two carbazole units substituted with a diphenylphosphine oxide, while CPBDC had an asymmetric molecular structure with one carbazole and one carbazole substituted with two diphenylphosphine oxide units. Both materials had the same molecular weight and were designed as the bipolar host material because they have hole transporting carbazole and electron transporting diphenylphosphine oxide groups. However, the difference in the molecular structure may affect the physical properties of BCPCB and CPBDC. Therefore, the photophysical properties of BCPCB and CPBDC were compared.

Physical properties of BCPCB and CPBDC are summarized in Fig. 1. UV-Vis absorption, PL and energy levels were measured. There was little difference in the UV-Vis and PL spectra between the two materials. The bandgaps calculated from the absorption edge of the UV-Vis absorption were 3.52 eV and 3.54 eV for BCPCB and CPBDC, respectively. The triplet energies of the two

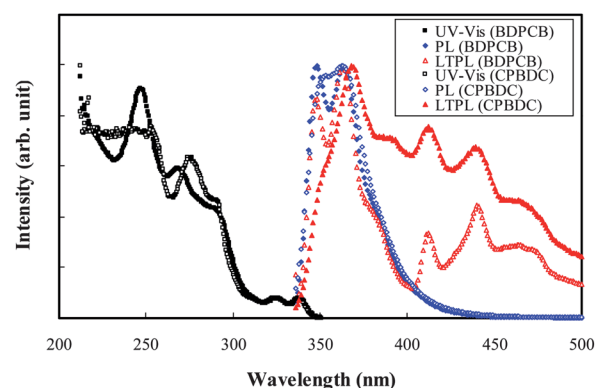


Fig. 1 UV-Vis and PL spectra of BCPCB and CPBDC.

host materials were 3.00 eV and 3.01 eV from low temperature PL spectra. The UV-Vis light is mostly absorbed by the carbazole unit and the diphenylphosphine oxide unit did not affect the UV-Vis absorption of the carbazole moiety. Therefore, similar UV-Vis spectra were obtained in BCPCB and CPBDC. The PL spectra were also similar because the PL emission was originated from the carbazole unit. The UV-Vis and PL emissions of BDPCB and CPBDC were quite similar to that of mCP. The bandgap of mCP from the absorption edge of UV-Vis spectra was 3.60 eV.

The highest occupied molecular orbital (HOMO) of host materials was measured using CV. CV curves of BCPCB and CPBDC are shown in Fig. 2. BCPCB showed an oxidation peak by the diphenylphosphine oxide substituted carbazole unit, while CPBDC showed an oxidation peak by the carbazole unit without any substituent among two carbazole groups. The introduction of the diphenylphosphine oxide group shifted the oxidation peak to high voltage due to strong electron withdrawing properties of the phosphine oxide group. The oxidation peak of CPBDC was similar to that of mCP, indicating that the oxidation is originated from the carbazole group without phosphine oxide units. The HOMO level of the BDPCB calculated from the onset of oxidation peak was -6.25 eV, while that of CPBDC was -6.13 eV. The LUMO level of the BDPCB calculated from the HOMO and the bandgap from UV-Vis was -2.73 eV, while the LUMO levels of CPBDC were -2.59 eV. The HOMO and LUMO of BDPCB were lowered compared to those of mCP by the strong electron withdrawing phosphine oxide unit. In the case

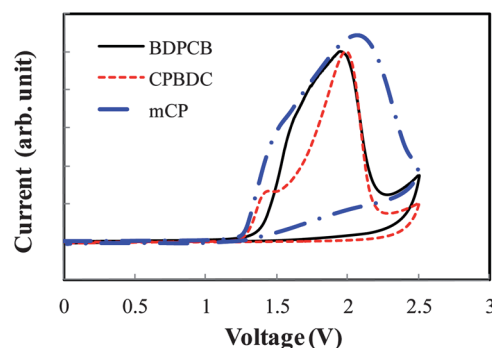


Fig. 2 Cyclic voltammometry curves of BCPCB and CPBDC.

of CPBDC, the HOMO was similar to that of mCP due to molecular orbital distribution.

Molecular orbital simulation of BCPCB and CPBDC was carried out to correlate the molecular orbital distribution with the HOMO and LUMO levels of BCPCB and CPBDC. The *ab initio* calculations were performed using a suite of Gaussian programs and the chemical structures of the host materials were fully optimized by density functional theory (DFT) using Becke's three parameterized Lee–Yang–Parr exchange functional (B3LYP) with 6-31G* basis sets.²³ Fig. 3 shows HOMO and LUMO distribution of BCPCB and CPBDC. The HOMO of CPBDC was mostly distributed over the unsubstituted carbazole, while the LUMO was concentrated on the carbazole substituted with two diphenylphosphine oxide groups. This

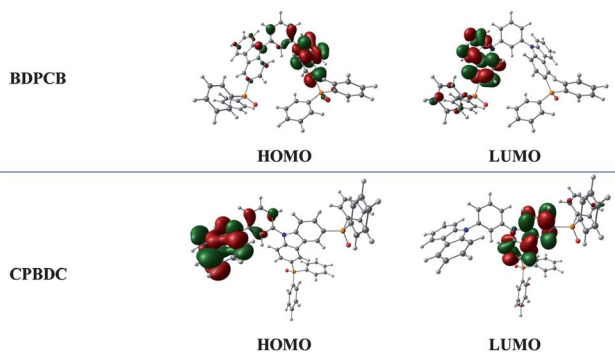


Fig. 3 Molecular orbital distribution of BCPCB and CPBDC.

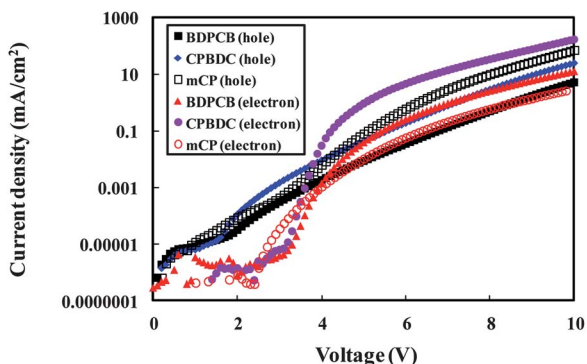


Fig. 4 Current density–voltage curves of the hole only and electron only devices.

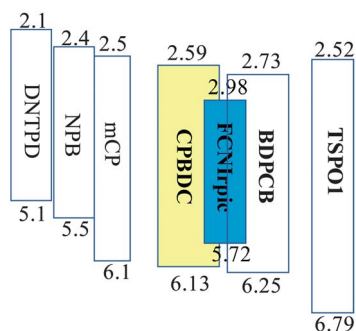


Fig. 5 Energy level diagram of the blue devices.

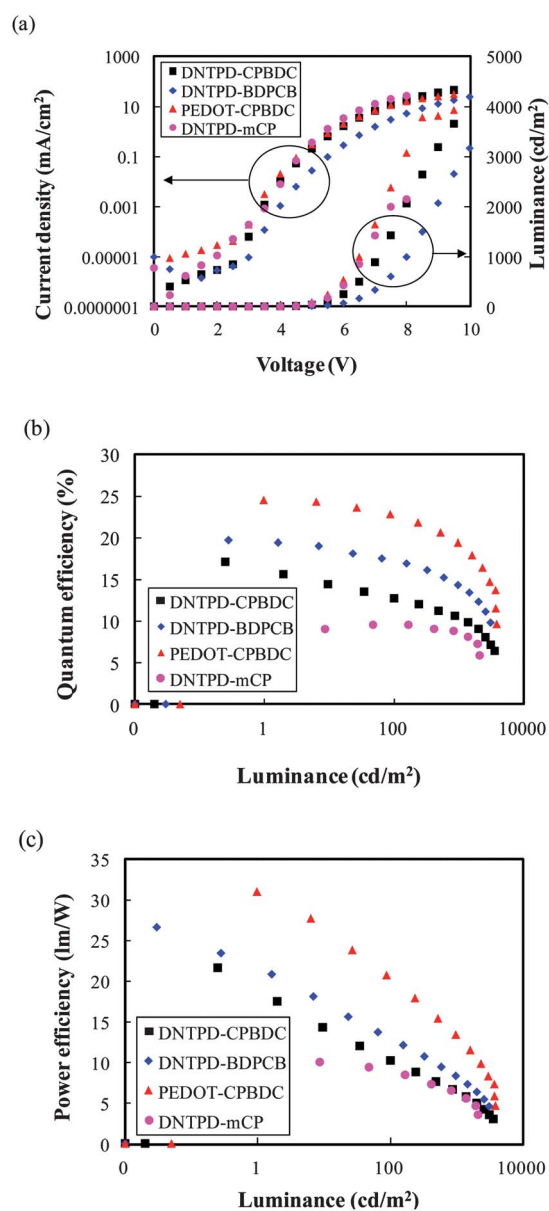


Fig. 6 Current density–voltage–luminance (a), quantum efficiency–luminance (b) and power efficiency–luminance (c) curves of BCPCB and CPBDC devices.

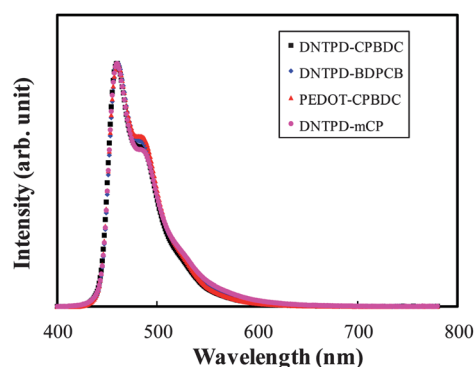


Fig. 7 Electroluminescence spectra of BCPCB and CPBDC devices.

Table 1 Device performances of BCPCB and CPBDC blue devices

	Driving voltage ^a /nm	Maximum quantum efficiency (%)	Quantum efficiency ^a (%)	Maximum power efficiency/lm W ⁻¹	Power efficiency ^a /lm W ⁻¹
DNTPD-BCPCB	8.0	19.7	14.3	23.4	8.3
DNTPD-CPBDC	7.2	17.1	10.3	21.6	6.1
PEDOT-CPBDC	6.5	24.5	19.4	31.0	13.4
DNTPD-mCP	6.7	9.5	8.5	10.0	6.1

^a Data were measured at 1000 cd m⁻².

indicates that the HOMO is dominated by the carbazole, while the LUMO is dominated by the diphenylphosphine oxide substituted carbazole. Compared with CPBDC, BCPCB showed simple orbital distribution as it has symmetric molecular structure. Both HOMO and LUMO were dispersed over the phosphine oxide substituted carbazole. The HOMO distribution of CPBDC explains the similar HOMO level to that of mCP. As the HOMO was localized on the same carbazole unit, there was little difference in HOMO levels between CPBDC and mCP.

The difference in the HOMO and LUMO levels between BCPCB and CPBDC may affect the hole and electron injection in the device. Therefore, hole only and electron only devices of blue PHOLEDs were fabricated. Fig. 4 shows current density–voltage curves of the hole only and electron only devices of BCPCB and CPBDC. The two host materials were designed as the bipolar host materials with two diphenylphosphine oxide groups in the molecular structure. However, both hole and electron current densities of CPBDC were higher than those of BCPCB. The high hole and electron current density of CPBDC can be explained by the HOMO and LUMO distribution of CPBDC. The hole current density is related to the HOMO level of the material. The HOMO level of CPBDC is more suitable for hole injection than that of BCPCB due to the HOMO level difference of 0.12 eV between BCPCB and CPBDC. In addition, the HOMO is mostly dispersed over the carbazole unit with good hole transport properties. The hole transport of BCPCB is dominated by the phosphine oxide substituted carbazole unit which is worse than the carbazole in terms of hole transport. Therefore, CPBDC showed higher hole current density. Similarly, the LUMO level and electron transport of CPBDC are determined by the carbazole unit substituted with two phosphine oxide groups compared with the carbazole unit substituted with one phosphine oxide group of BCPCB. The additional phosphine oxide group of CPBDC enhances the electron current density of CPBDC. The asymmetrically designed CPBDC showed good hole transport properties due to the carbazole group and good electron transport properties owing to the carbazole group substituted with two diphenylphosphine oxide units. The asymmetric design was better than the symmetric design in terms of hole and electron transport properties. Compared with mCP with good hole transport and poor electron transport properties, the two host materials showed higher electron current density and lower hole current density. This proves that the phosphine oxide substituents improved the electron transport properties of BDPCB and CPBDC. Therefore, BDPCB and CPBDC were more suitable as the bipolar host material than mCP. The energy level diagram of the materials is shown in Fig. 5.

Deep blue PHOLEDs were fabricated using BCPCB and CPBDC as the host materials. Fig. 6 shows device performances of the deep blue PHOLED with BCPCB and CPBDC host materials. The current density of the CPBDC device was higher than that of the BCPCB device. As shown in the hole only and electron only device data, the high hole and electron current density of the CPBDC device enhanced the current density of the device because of efficient hole and electron injection. The luminance was also increased due to more charge injection. However, the quantum efficiency was high in the BCPCB device. The efficiency is determined by the charge balance in the emitting layer and the BCPCB device was better than CPBDC in terms of recombination efficiency. Although CPBDC showed high current density, the electron density of the CPBDC device was much higher than the hole density, resulting in rather poor charge balance in the emitting layer.

Therefore, the device structure of the CPBDC device was further optimized. PEDOT:PSS was used instead of DNTPD and the thickness of the electron transport layer was changed from 15 nm to 25 nm. The quantum efficiency was greatly improved by optimizing the device structure and a maximum quantum efficiency of 24.5% was obtained from the CPBDC device. The quantum efficiency was not degraded even at high luminance and a quantum efficiency of 19.4% was achieved at 1000 cd m⁻². The power efficiency was also high in the CPBDC device and the maximum power efficiency and power efficiency at 1000 cd m⁻² were 31.0 lm W⁻¹ and 13.4 lm W⁻¹. The low driving voltage and high quantum efficiency yielded high power efficiency in the CPBDC device with the PEDOT:PSS hole injection layer. The quantum and power efficiencies of CPBDC and BDPCB devices were much higher than those of the mCP device. This is due to bipolar charge transport properties of CPBDC and BDPCB.

The electroluminescence spectra are shown in Fig. 7 and the peak maximum of the spectra was 462 nm. The color coordinate of the deep blue PHOLEDs was (0.14, 0.19). All device data of deep blue PHOLEDs are summarized in Table 1.

Conclusions

In conclusion, symmetric and asymmetric bipolar host materials were systematically compared as the host materials for deep blue PHOLEDs. The asymmetric design was better than the symmetric design in terms of device performances. The driving voltage could be lowered due to efficient hole and electron injection and high quantum efficiency could be achieved. A high quantum efficiency of 24.5% and power efficiency of 31.0 lm W⁻¹ could be obtained from deep blue PHOLEDs with the CPBDC

high triplet energy host material. The asymmetric molecular design can be useful to improve the driving voltage and quantum efficiency in phosphorescent devices.

Notes and references

- 1 T. Sajoto, P. I. Djurovich, A. Tamayo, M. Yousufuddin, R. Bau, M. E. Thompson, R. J. Holmes and S. R. Forrest, *Inorg. Chem.*, 2005, **44**, 7992–8003.
- 2 P. Erk, M. Bold, M. Egen, E. Fuchs, T. Geßner, K. Kahle, C. Lennartz, O. Molt, S. Nord, H. Reichelt, C. Schildknecht, H.-H. Johannes and W. Kowalsky, *Dig. Tech. Pap. - Soc. Inf. Disp. Int. Symp.*, 2006, **37**, 131–134.
- 3 R. J. Holmes, S. R. Forrest, T. Sajoto, A. Tamayo, P. I. Djurovich, M. E. Thompson, J. Brooks, H. J. Tung, B. W. D'Andrade, M. S. Weaver, R. C. Kwong and J. J. Brown, *Appl. Phys. Lett.*, 2005, **87**, 243507.
- 4 C.-F. Chang, Y.-M. Cheng, Y. Chi, Y.-C. Chiu, C.-C. Lin, G.-H. Lee, P.-T. Chou, C.-C. Chen, C.-H. Chang and C.-C. Wu, *Angew. Chem., Int. Ed.*, 2008, **47**, 4542–4545.
- 5 S. H. Kim, J. Jang, S. J. Lee and J. Y. Lee, *Thin Solid Films*, 2008, **517**, 722–726.
- 6 K. S. Yook, S. O. Jeon, C. W. Joo and J. Y. Lee, *Org. Electron.*, 2009, **10**, 170–173.
- 7 R. J. Holmes, S. R. Forrest, Y.-J. Tung, R. C. Kwong, J. J. Brown, S. Garon and M. E. Thompson, *Appl. Phys. Lett.*, 2003, **82**, 2422–2424.
- 8 M. H. Tsai, H. W. Lin, H. C. Su, T. H. Ke, C. C. Wu, F. C. Fang, Y. L. Liao, K. T. Wong and C. I. Wu, *Adv. Mater.*, 2006, **18**, 1216–1220.
- 9 M. F. Wu, S. J. Yeh, C. T. Chen, H. Murayama, T. Tsuboi, W. Li, I. Chao, S. Liu and J. K. Wang, *Adv. Funct. Mater.*, 2007, **17**, 1887–1895.
- 10 R. J. Holmes, B. W. D'Andrade, S. R. Forrest, X. Ren, J. Li and M. E. Thompson, *Appl. Phys. Lett.*, 2003, **83**, 3818–3820.
- 11 X. Ren, J. Li, R. J. Holmes, P. I. Djurovich, S. R. Forrest and M. E. Thompson, *Chem. Mater.*, 2004, **16**, 4743–4747.
- 12 A. B. Padmaperuma, L. S. Sapochak and P. E. Burrows, *Chem. Mater.*, 2006, **18**, 2389.
- 13 S. O. Jeon, K. S. Yook, C. W. Joo and J. Y. Lee, *Adv. Funct. Mater.*, 2009, **19**, 3644.
- 14 S. O. Jeon, K. S. Yook, C. W. Joo and J. Y. Lee, *Adv. Mater.*, 2010, **22**, 1872.
- 15 S. O. Jeon, S. E. Jang, H. S. Son and J. Y. Lee, *Adv. Mater.*, 2011, **23**, 1436.
- 16 L. S. Sapochak, A. B. Padmaperuma, X. Cai, J. L. Male and P. E. Burrows, *J. Phys. Chem. C*, 2008, **112**, 7989.
- 17 P. K. Koech, E. Polikarpov, J. E. Rainbolt, L. Cosimbescu, J. S. Swensen, A. L. Von Ruden and A. B. Padmaperuma, *Org. Lett.*, 2010, **12**, 5534.
- 18 M. Rothmann, S. Haneder, E. D. Como, C. Lennartz, C. Schildknecht and P. Stroehriegel, *Chem. Mater.*, 2010, **22**, 2403.
- 19 K. Son, M. Yahiro, T. Imai, H. Yoshizaki and C. Adachi, *Chem. Mater.*, 2008, **20**, 4439.
- 20 S.-J. Su, H. Sasabe, T. Takeda and J. Kido, *Chem. Mater.*, 2008, **20**, 1691.
- 21 J. Ding, Q. Wang, L. Zhao, D. Ma, L. Wang, X. Jing and F. Wang, *J. Mater. Chem.*, 2010, **20**, 8126.
- 22 F.-M. Hsu, C.-H. Chien, P.-I. Shih and C.-F. Shu, *Chem. Mater.*, 2009, **21**, 1017.
- 23 M. J. Frisch, G. W. Trucks, H. B. Schlegel, G. E. Scuseria, M. A. Robb, J. R. Cheeseman, J. A. Montgomery, T. Vreven, Jr, K. N. Kudin, J. C. Burant, J. M. Millam, S. S. Iyengar, J. Tomasi, V. Barone, B. Mennucci, M. Cossi, G. Scalmani, N. Rega, G. A. Petersson, H. Nakatsuji, M. Hada, M. Ehara, K. Toyota, R. Fukuda, J. Hasegawa, M. Ishida, T. Nakajima, Y. Honda, O. Kitao, H. Nakai, M. Klene, X. Li, J. E. Knox, H. P. Hratchian, J. B. Cross, C. Adamo, J. Jaramillo, R. Gomperts, R. E. Stratmann, O. Yazyev, A. J. Austin, R. Cammi, C. Pomelli, J. W. Ochterski, P. Y. Ayala, K. Morokuma, G. A. Voth, P. Salvador, J. J. Dannenberg, V. G. Zakrzewski, S. Dapprich, A. D. Daniels, M. C. Strain, O. Farkas, D. K. Malick, A. D. Rabuck, K. Raghavachari, J. B. Foresman, J. V. Ortiz, Q. Cui, A. G. Baboul, S. Clifford, J. Cioslowski, B. B. Stefanov, G. Liu, A. Liashenko, P. Piskorz, I. Komaromi, R. L. Martin, D. J. Fox, T. Keith, M. A. Al-Laham, C. Y. Peng, A. Nanayakkara, M. Challacombe, P. M. W. Gill, B. Johnson, W. Chen, M. W. Wong, C. Gonzalez and J. A. Pople, *Gaussian 03, revision B05*, Gaussian, Inc., Pittsburgh, PA, 2003.